Self-Assembly of Tethered Diblocks in Selective Solvents

Ekaterina B. Zhulina,[†] Chandralekha Singh,[†,‡] and Anna C. Balazs*[,†]

Chemical and Petroleum Engineering Department and Physics and Astronomy Department, University of Pittsburgh, Pittsburgh, Pennsylvania 15261

Received April 30, 1996; Revised Manuscript Received September 3, 1996[⊗]

ABSTRACT: We use scaling arguments and self-consistent field calculations to determine the behavior of AB diblock copolymers that are grafted to a planar surface at relatively low densities. The surrounding solution is assumed to be a theta or marginally good solvent for the A block and a poor solvent for the B block. When the chains are grafted by the ends of the B blocks and the B blocks are sufficiently long, the layer associates into an ordered array of "flowerlike" structures. The solvophobic B's form the core of the "flowers", and the soluble A's form the outer corona of "petals". The size and spacing of the micellar aggregates can be manipulated by varying the different block lengths. The findings provide guidelines for fabricating patterned films with well-defined morphologies.

Introduction

Tethering copolymers at fluid/fluid[1] or fluid/solid interfaces[2,3] provides a novel means of creating patterned films with well-defined morphologies. Patterned films can potentially be useful in fabricating a variety of optoelectronic devices.[4] Ordered substrates can also be used as micro "reaction vessels", where various chemical reactions can occur simultaneously in different domains across the substrate.[5] If the films are composed of both hydrophilic and hydrophobic domains, the surface can be used as a template for growing biological cells with well-defined shapes and sizes.[6] To optimize the utility of these films, it is important to isolate the factors that control the structure of the layer and establish guidelines for tailoring the size and shape of the structures.

With this aim in mind, we recently used theoretical models to investigate the behavior of diblock copolymers tethered onto a solid surface.[3] The studies revealed that at relatively sparse grafting densities and in poor solvents, the diblocks self-assemble into an ordered layer of pinned micelles.[7,8] Depending on the values of the polymer−polymer and polymer−solvent interaction parameters, the micelles resemble "onion"-, "garlic"-, or "dumbbell"-like structures.[3] In the onion-like micelles, the less solvophobic blocks form an outer layer that encircles the more solvophobic segments. In the garlics, the highly solvophobic core splits into multiple, smaller cores, which are encapsulated in an outer layer. The dumbbells consist of two distinct cores, with one being atop the other. The studies also showed how the sizes and periodicities of these structures depend on the molecular weights of the blocks, their relative solvent affinity, and the grafting density.[3]

In this paper, we continue our investigations into the self-assembly of tethered diblocks. We now focus on the case where the solvent acts as a theta or good solvent for one block but is a poor solvent for the other. Under these conditions, it is anticipated that the self-assembly of the layer will be affected by the swelling of the solvophilic component, and the morphology of the film will be quite different from that formed by two distinctly solvophobic blocks.

In examining the equilibrium structure of the tethered layer, we use two complementary theoretical techniques: two-dimensional self-consistent field (SCF) calculations[3,9−12] and scaling arguments. Below, we first present the results of the scaling analysis and then describe the SCF findings on the comparable system.

The System

We consider flexible diblock copolymers that are tethered onto a planar surface by the end of one of the blocks. The blocks contain N_A and N_B symmetric monomer units of size a and the grafting density is $1/s$, where s is the area per chain. We assume that the surrounding solution is a theta or a marginally good solvent for the A blocks, i.e., $\tau_A = (T - \Theta_A)/T \geq 0$ and a poor solvent for the B blocks, i.e., $\tau_B = (\Theta_B - T)/T > 0$ and $N_B\tau_B^2 \gg 1$. Here, Θ_A and Θ_B are the corresponding theta temperatures for the components of the diblock. As before,[3] we examine two separate cases: (1) the chains are grafted by the end of the A block, and (2) the chains are grafted by the end of the B block. We also assume that neither block adsorbs on the substrate (both components totally dewet the surface).

Chains Tethered by the Soluble A Block. *Scaling Analysis.* We focus on grafting densities described by $(N_B^{1/2}/\tau) < s/a^2 < N_B^{4/3}\tau^{2/3}$. Within this range,[7] when N_A is small, the B blocks form pinned micelles, where the A blocks are incorporated into the micelles' "legs", the segments that tether the micellar core to the substrate. On the other hand, when N_A is relatively large, the well-solvated A blocks form a brush; the height of this brush is given by $H \sim N_A$. We consider the latter case first and then examine the effect of decreasing N_A. We note that in formulating the scaling expressions below, we omit all numerical coefficients on the order of unity.

For large values of N_A ($\gg s/a^2$), the less soluble B component is located at the edge of the planar brush formed by the swollen A blocks. The solvophobic interactions drive the B blocks to self-assemble and form B micelles that are located at the top of the A brush. The expression for the free energy of this layer contains the following contributions,

$$\Delta F = \Delta F_s + \Delta F_B + \Delta F_A \quad (1)$$

Here, the ΔF_s term is given by

$$\Delta F_s = \tau_B^2 R_B^2/f \quad (2)$$

where f is the number of chains within the micelles and

[†] Materials Science and Engineering Department.
[‡] Physics and Astronomy Department.
[⊗] Abstract published in *Advance ACS Abstracts,* November 1, 1996.

S0024-9297(96)00642-0 CCC: $12.00

ΔF_s is the surface free energy (in units of kT) associated with the core of a micelle whose radius is given by

$$R_B = a(fN_B/\tau_B)^{1/3} \quad (3)$$

The ΔF_B term

$$\Delta F_B = R_B{}^2/a^2 N_B \quad (4)$$

accounts for stretching of the B blocks in the core of the micelle. The ΔF_A term represents the losses in free energy due to the lateral and normal stretching of the A blocks and the "repulsive" intermolecular interactions between the A units. The particular form of ΔF_A depends on the values of N_A. For long A blocks ($H \gg D$), the system can be viewed as a planar brush of thickness H, covered by spherical micelles whose size is given by $D = (fs/a^2)^{1/2}$. Correspondingly

$$\Delta F_A = \Delta F_{A,brush} + \Delta F_{A,micelle} \quad (5)$$

where the terms on the right describe the free energy losses associated with the A segments in the brush and in the corona of the micelle, respectively. The particular expressions for H and ΔF_A also depend on the solvent quality, τ_A. Here, we assume $\tau_A = 0$, or theta solvent conditions. Generalizing the expressions to good solvent conditions, or $\tau_A > 0$, is straightforward. Under theta and good solvent conditions, the free energy of a chain in the corona of a spherical micelle is (neglecting logarithmic prefactors):[13,14]

$$\Delta F_{A,micelle} = f^{1/2} \quad (6)$$

Gathering all the terms, the total free energy per chain, ΔF, can now be written as

$$\Delta F = \tau_B{}^{4/3} N_B{}^{2/3}/f^{1/3} + f^{2/3}/\tau_B{}^{2/3} N_B{}^{1/3} + f^{1/2} + \Delta F_{A,brush} \quad (7)$$

To determine the equilibrium characteristics of the system, we minimize this ΔF with respect to f, the number of chains within the micelles. Since $\Delta F_{A,brush}$ does not depend on f, we can ignore this contribution to eq 7. Furthermore, at $\tau_B{}^2 N_B \gg 1$, the stretching of B blocks in the core is negligible with respect to that of the A segments in the corona. Hence, we can also neglect the second term in eq 7. Thus, the equilibrium characteristics are determined by the balance of the corona contribution and the surface free energy. Minimizing the sum of the first and third terms with respect to f, we obtain

$$f = (\tau_B{}^2 N_B)^{4/5} \quad (8)$$

Substituting this value of f into eq 3, we find that the radius of the core R_B scales as

$$R_B = a\tau_B{}^{1/5} N_B{}^{3/5} \quad (9)$$

whereas the periodicity $D = a(fs/a^2)^{1/2}$ is given by

$$D = a\tau_B{}^{4/5} N_B{}^{2/5} (s/a^2)^{1/2} \quad (10)$$

As seen from eqs 8−10, f, R_B, and D do not scale with N_A. The molecular weight dependences of R_B and f on N_B coincide with those for "starlike" block copolymer micelles in solution.[15,16] For starlike micelles, the insoluble B core is much smaller than the A corona.

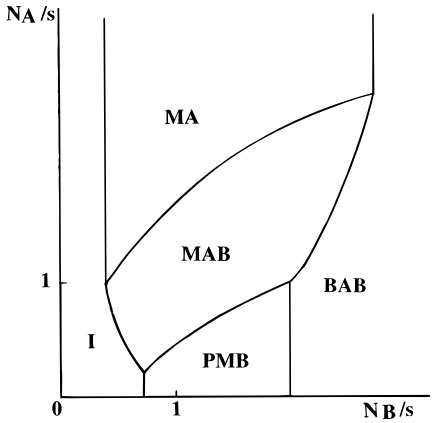

Figure 1. Diagram of states for the system in the N_A/s and N_B/s coordinates. The various regions are discussed in the text.

With decreases in N_A, the elasticity of the A blocks plays a more crucial role in determining the structure of the layer. Under theta solvent conditions, the brush thickness $H = aN_A(s/a^2)^{-1/2}$ becomes comparable to D, eq 10, at $N_A \sim \tau_B{}^{4/5} N_B{}^{2/5} s/a^2$. Further decreases in N_A lead to a structural rearrangement of the layer. Though the layer around the B cores remains spherical, the A blocks become significantly stretched in the lateral direction. Here, $H \ll D$, and the elastic contribution from the A block yields

$$\Delta F_A = D^2/a^2 N_A \quad (11)$$

Now, the structure of the micelles is determined by a balance of the surface free energy of the core, eq 2, and the elasticity of the blocks A, eq 11. Minimizing the sum of these two terms with respect to f gives

$$f = \tau_B N_B{}^{1/2} N_A{}^{3/4}/(s/a^2)^{3/4} \quad (12)$$

Correspondingly, the radius R_B and the periodicity D scale as

$$R_B = aN_B{}^{1/2} N_A{}^{1/4}/(s/a^2)^{1/4} \quad (13)$$

$$D = a\tau_B{}^{1/2} N_B{}^{1/4} N_A{}^{3/8} (s/a^2)^{1/8} \quad (14)$$

From eqs 12−14, we see that a decrease in N_A leads to a reduction in the size of the micelles and an increase in the lateral tension within the A blocks, which is given by $D/N_A = \tau_B{}^{1/2} N_B{}^{1/4} N_A{}^{-5/8} (s/a^2)^{1/8}$. Depending on the range of N_B values, one can envision two scenarios. If $N_B > \tau_B{}^2 (s/a^2)$, a decrease in N_A leads to a merging of the micellar cores and the formation of a continuous B layer.

If, however, $N_B < \tau_B{}^2 (s/a^2)$, a decrease in N_A leads to a noticeable increase in the lateral tension, D/N_A, in the A blocks. When this tension becomes comparable to τ_B, the B monomers are pulled out of the core and pulled into the micellar legs. Further decreases in N_A lead to a reduction in the fraction of A units within the legs (at a fixed value of tension, τ_B). Here, the legs can be envisioned as strings of blobs of size a/τ_B (see ref 17 for further details), and their elasticity is now given by

$$\Delta F_B = \tau_B D = \tau_B f^{1/2} (s/a^2)^{1/2} \quad (15)$$

Balancing eq 15 with the surface free energy of the core, eq 2, we arrive at the conventional dependences for

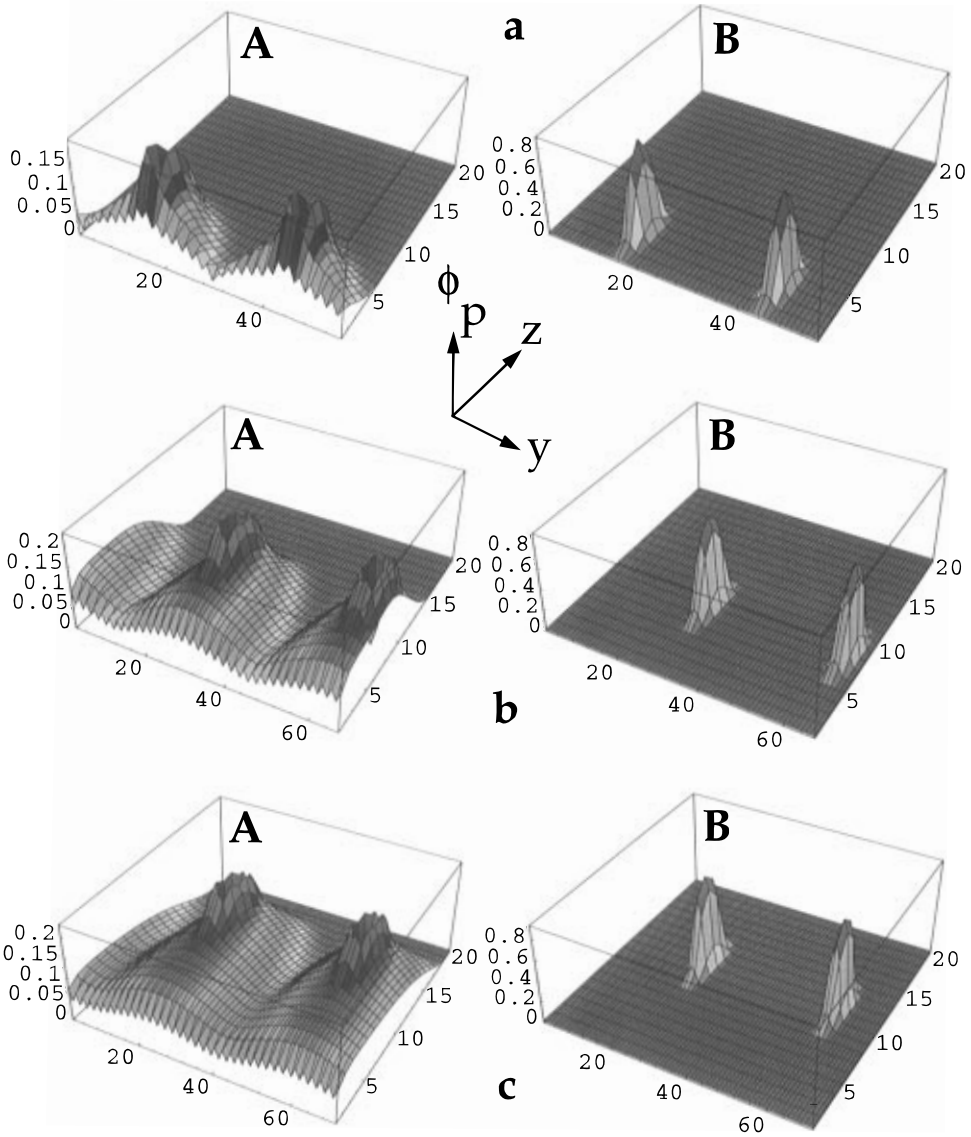

Figure 2. Three-dimensional plots showing the effect of increasing N_A while keeping N_B fixed at 20 for diblock copolymers grafted by the soluble A block: (a) $N_A = 30$, (b) $N_A = 80$, and (c) $N_A = 120$. The grafting density per line ρ is 0.025, $\chi_{BS} = 2$, $\chi_{AS} = 0$, and $\chi_{AB} = 0$. *Y* refers to the grafting direction and ϕ_p is the polymer density. The plots marked B show the polymer density of B blocks, while the plots marked A show the density of A blocks.

pinned micelles formed by the pure B component

$$f = \tau_B^{2/5} N_B^{4/5}/(s/a^2)^{3/5} \tag{16}$$

$$R_B = a N_B^{3/5}/(\tau_B s/a^2)^{1/5} \tag{17}$$

$$D = a N_B^{2/5}(\tau_B s/a^2)^{1/5} \tag{18}$$

Diagram of States. The above results are summarized in the scaling "diagram of states" plotted in N_A/s vs N_B/s coordinates (Figure 1). The lines separating the various regions mark the locations of the crossover between the different morphologies. (With our scaling approach, we cannot specify whether these lines indicate regions of continuous crossover or mark abrupt transitions.) The central part of the diagram encompasses the regimes discussed above: the MA regime of starlike block copolymer micelles (eqs 8−10), the MAB regime where the legs of the micelles are formed by the blocks A (eqs 12−14), and the PMB regime of pinned micelles formed by "pure" B (eqs 16−18).

To the left of these regimes (at very sparse grafting), one finds the regime of nonaggregating chains, I. Depending on the length of the A segments, the collapsed B blocks sit atop nonoverlapping A coils ($N_A/s < 1$), or atop stretched chains formed by long A blocks ($N_A/s > 1$). In both cases, there is no lateral self-assembling in the system. The boundaries between the regime I and the micelles regimes MA, MAB, and PMB are found by setting $f = 1$ in the corresponding eqs 8, 12, and 16.

To the right of the micelle regimes (at relatively high grafting densities), one finds the regime BAB where both components A and B form continuous layers. The corresponding boundaries with the regimes MA, MAB, and PMB are found by setting $R_B = D$ in eqs 9, 10, 13, 14, and 17, 18, respectively.

Self-Consistent Field Theory. To visualize the structure of the self-assembled layers described above, we turn to self-consistent field (SCF) theory. Our self-consistent field method is based on that developed by Scheutjens and Fleer,[18] which in turn is based on a Flory−Huggins approach, combining Markov chain statistics with a mean-field approximation. The equations in this model are solved numerically and self-consistently. The self-consistent potential is a function

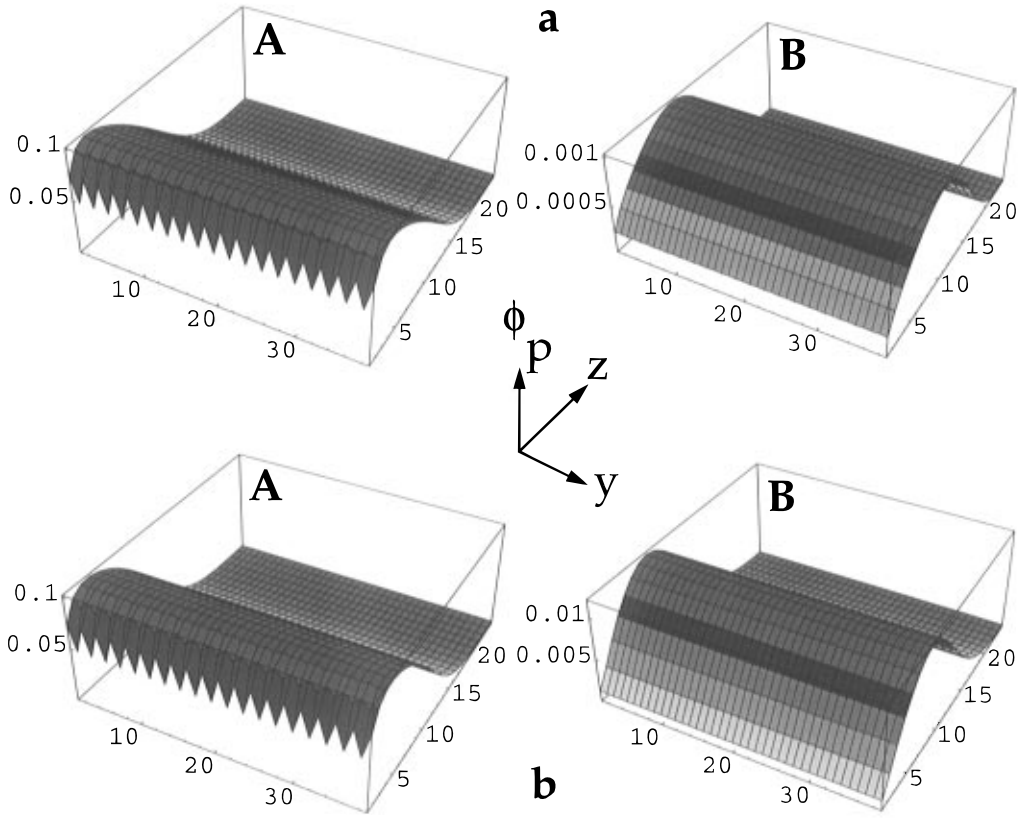

Figure 3. Three-dimensional plots showing the self-assembly for $N_A = 80$ and two values of N_B, where N_B is small. The diblock copolymers are grafted by the soluble A block. In (a), $N_B = 1$ and in (b), $N_B = 10$. The grafting density per line ρ is 0.025, $\chi_{BS} = 2$, $\chi_{AS} = 0$, and $\chi_{AB} = 0$. Y refers to the grafting direction and ϕ_p denotes the polymer density. The plots marked B show the polymer density of B blocks, while the plots marked A show the density of A blocks.

of the polymer segment density distribution and the Flory−Huggins interaction parameters. The calculations yield the equilibrium density profiles for the grafted polymers. These density profiles provide a picture of the local concentration gradients in the system.

In the one-dimensional SCF theory, the segment density distribution only depends on Z, the direction perpendicular to the surface. This 1D model is insufficient for capturing the lateral heterogeneities that appear within the layer when the chains are immersed in a poor solvent. We therefore use a two-dimensional SCF theory, where the density distribution depends on *both* the Y and Z directions. (The model has been amply described elsewhere and we refer the reader to refs 3 and 9−12 for further details.) The system is assumed to be translationally invariant along X, the mean field direction. Therefore, the micelles form cylindrical structures along the X-axis. However, the qualitative behavior exhibited by this system will be similar to that formed by spherical micelles. Due to these differences in geometry, we do not use the SCF model to test the scaling predictions obtained for the spherical structures. Rather, the SCF calculations allow us to visualize and obtain insight into the changes that occur as we vary the system parameters.

The calculations are performed on a cubic lattice and the ends of the chains are grafted to the $Z = 1$ plane, which represents a flat, impenetrable surface. Periodic boundary conditions are applied along Y. The chains are grafted at every alternate lattice site along the Y direction. The parameter ρ gives the grafting density per line along X. (This implies that the average spacing between points along a line in X is $1/\rho$ and the area per chain is $s = 2/\rho$.) We fix $\rho = 0.025$ and set the polymer−solvent interaction parameters for the A and B blocks to $\chi_{AS} = 0$ and $\chi_{BS} = 2$, respectively. The block−surface interaction is taken to be the same as the block−solvent interaction.

We first examine the case where the chains are grafted by the ends of the soluble A blocks. Figure 2 displays the graphical output from the SCF calculations. The figures reveal the structural changes that occur when the length of the A block is gradually increased, while the B block length is held fixed at $N_B = 20$. This choice of parameters corresponds to taking a vertical cross section of the phase diagram in Figure 1 at $N_B = 20$.[19] When the length of the soluble A block is small (e.g., $N_A = 10$ or 20), the layer is laterally homogeneous. Here, the chains are too short to stretch and associate into multichain aggregates. However, when N_A is increased to 30 or 40 lattice sites, the chains self-assemble and the B blocks form pronounced micelles (Figure 2a). As can be seen from the figure, the A blocks stretch in the lateral direction and form a coating or shell around the B cores. The A coating shields the B's from the unfavorable solvent and thereby lowers the interfacial tensions in the system.[3]

When the length of the soluble blocks is increased further, the A's form a polymer brush. The density of A's, however, is not monotonic in the normal direction; it is higher around the B cores since the A's shield this solvophobic region. If the increase in N_A is continued, the height of the A layer increases monotonically, as expected for planar brushes, and the micelles formed by the B blocks move farther away from the grafting surface (Figure 2b,c). We note that the shielding of the B micelles by the A blocks becomes more pronounced as N_A is initially increased (compare parts a and b of Figure 2) but remains unchanged once N_A is sufficiently

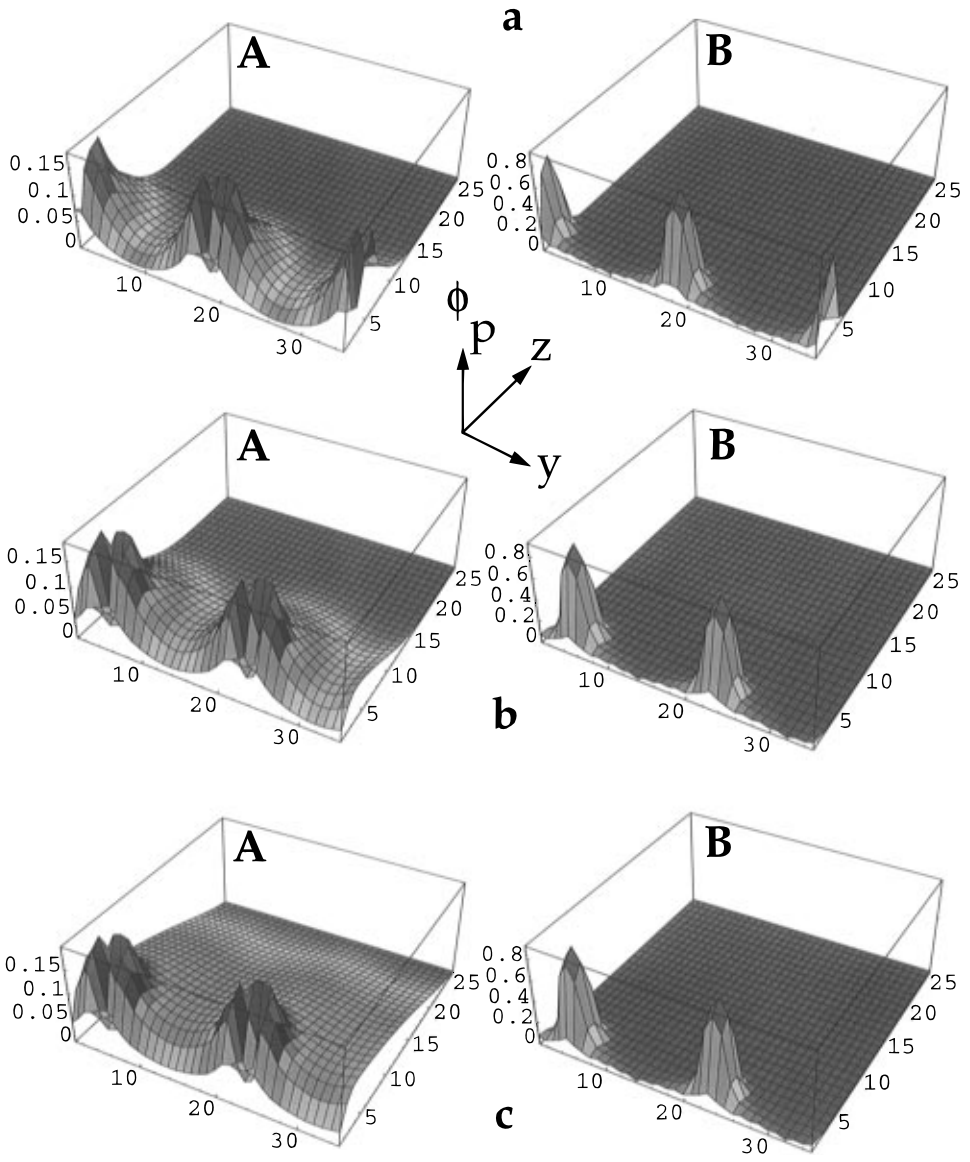

Figure 4. Three-dimensional plots showing the effect of increasing N_A while keeping N_B fixed at 40 for diblock copolymers by the solvophobic B blocks: (a) $N_A = 40$, (b) $N_A = 100$, and (c) $N_A = 160$. The grafting density per line ρ is 0.025, $\chi_{BS} = 2$, $\chi_{AS} = 0$, and $\chi_{AB} = 0$. Y refers to the grafting direction and ϕ_p denotes the polymer density. The plots marked B show the polymer density of B blocks, while the plots marked A show the density of A blocks.

large to form brushes (compare parts b and c of Figure 2). In addition, the number of chains within each micelle, or f, slowly increases with initial increases in N_A but shows negligible change when $N_A \sim 100$.

We note that if N_B is very small ($N_B \leq 10$), the layer is uniform in the lateral direction and micelles are not formed.[20,21] Instead, the diblocks form stretched brushes where the B blocks follow the usual distribution for chain ends.[20] The three-dimensional plots in Figure 3a,b illustrate this situation for $N_A = 80$ and for values of $N_B = 1$ and 10, respectively. The polymer density ϕ_p of the B chains is obviously lower for $N_B = 1$ than $N_B = 10$ since there are more B monomers in the latter case. The overall results are consistent with the scaling predictions discussed earlier.

Chains Tethered by the Less Soluble B Block. *Scaling Analysis.* In the case where the chains are tethered by the end of the B blocks, the self-assembled structures resemble flowers (see Figure 4). Here, the solvophobic B's form the core and the legs of the micelles (strings of the thermal blobs of size $\xi = a/\tau_B$), and the swollen A blocks form a spherical brush that decorates the cores. The characteristics of the micelles are only slightly affected by the presence of the A blocks. The free energy per chain in such a micelle is given by

$$\Delta F = \Delta F_B + \Delta F_s + \Delta F_A \tag{19}$$

where ΔF_B and ΔF_s are given by eqs 15 and 2, respectively, whereas ΔF_A is the free energy of the spherical brush, eq 6. The total free energy per chain is then given by

$$\Delta F_A = \tau_B (fs/a^2)^{1/2} + \tau_B^{4/3} N_B^{2/3}/f^{1/3} + f^{1/2} \tag{20}$$

At $\tau_B(s/a^2)^{1/2} \gg 1$ (or $\xi \ll s^{1/2}$), the last term in eq 20 is always smaller than the first term, which describes the stretching of the micellar legs. Thus, balancing the surface free energy of the core and the elasticity of the legs (that is, minimizing the first and second terms in eq 20 with respect to f), one arrives at the familiar dependences in eqs 16−18 that characterize pinned micelles of "pure" B.

The thickness of the spherical outer shell, H, is given by[13,14]

$$H = a\tau_A^{1/5} N_A^{3/5} f^{1/5} \quad (21)$$

in good solvent conditions, and by

$$H = aN_A^{1/2} f^{1/4} \quad (22)$$

in theta solvent conditions. When the neighboring shells start to overlap ($H = D$), the spherical geometry of the shells transforms into a planar geometry.[22] Further increases in N_A lead to the formation of a brush that displays rather unusual modulations of the polymer concentration in the lateral direction. Near the surface, the B blocks form pinned micelles; moving away from the surface, the lateral modulations in the A profile disappear, and the brush becomes laterally uniform near the edge of the layer.

Self-Consistent Field Theory. In Figure 4, we plot the data for the 2D SCF calculations on the flowerlike structures that are formed when the solvophobic component B is grafted onto the planar surface. Results are shown for $N_A = 40$, 100, and 160, while N_B is held fixed at 40. The solvent-incompatible B blocks form a dense micellar core and the soluble A blocks form a shield around the B micelles. Again, this A coating reduces the extent of B-solvent contact. Thus, the structure resembles a "flower" whose core is formed by the B blocks and the "petals" are formed by the A blocks.

As the length of the A block is increased, the solvent-shielding layer remains unchanged and the rest of the A blocks form a stretched layer, or brush (Figure 4, b and c). With further increases in N_A, the brush extends to larger distances in the Z direction. The position of the micelle, the polymer density within the core, and the number of chains in the micelle are unaffected by the increase in N_A, in agreement with the above scaling predictions.

Conclusions

To summarize, we used both scaling arguments and SCF calculations to analyze the structure of tethered diblocks in selective solvents. The detailed morphology of these structures depends on the composition of the block copolymer and the manner in which the chains are grafted onto the surface (that is, whether they are tethered by the solvophilic or solvophobic block).

We note that if the grafting is relatively uniform, the diblocks will form an ordered array or pattern on the surface. The advantage of forming patterned films with tethered copolymers is that the size and spacing of the micelles, and thus the dimensions of the pattern, can be controlled by varying the chain length, solvent quality, or grafting density. With the ability to control the size of the patterns, the films can be tailored for specific applications, including coatings for optoelectronic devices.

Acknowledgment. A.C.B. graftefully acknowledges financial support from the Materials Research Center, funded by AFOSR, through grant No. F49620-95-1-0167, and NSF for financial support through grant DMR-94-07100. C.S. also gratefully acknowledges financial support from NSF grant DMR-92-17935 to D. M. Jasnow.

References and Notes

(1) Zhu, J.; Eisenberg, A.; Lennox, R. B. J. *Am. Chem. Soc.* **1991**, *113*, 5583; *Langmuir* **1991**, *7*, 1579; *J. Phys. Chem.* **1992**, *96*, 4727; *Macromolecules* **1992**, *25*, 6547.
(2) Zhulina, E.; Balazs, A. C. *Macromolecules* **1996**, *29*, 2667.
(3) Zhulina, E.; Singh, C.; Balazs, A. C. *Macromolecules* **1996**, *29*, 6338.
(4) Dagani, R. *Chem. Eng. News* **1996**, *March 4*, 22.
(5) Borman, S. *Chem. Eng. News* **1996**, *Feb 12*, 29.
(6) Singhvi, R., et al. *Science* **1994**, *264*, 696.
(7) Klushin, L. I., unpublished work.
(8) Williams, D. R. M. *J. Phys. II* **1993**, *3*, 1313.
(9) Huang, K.; Balazs, A. C. *Phys. Rev. Lett.* **1991**, *66*, 620. Huang, K.; Balazs, A. C. *Macromolecules* **1993**, *26*, 4736. Yeung, C.; Huang, K.; Jasnow, D.; Balazs, A. C. *Colloids Surf.* **1994**, *86*, 111.
(10) Israels, R.; Gersappe, D.; Fasolka, M.; Roberts, V. A.; Balazs, A. C. *Macromolecules* **1994**, *27*, 6679. Balazs, A. C.; Gersappe, D.; Israels, R.; Fasolka, M. *Macromol. Theory Simul.* **1995**, *4*, 585.
(11) Singh, C.; Balazs, A. C. *J. Chem. Phys.* **1996**, *105*, 706.
(12) Singh, C.; Zhulina, E.; Gersappe, D.; Pickett, G.; Balazs, A. C. *Macromolecules* **1996**, *29*, 7637.
(13) Daoud, M.; Cotton, J. P. *J. Phys.* **1982**, *43*, 531.
(14) Birshtein, T. M.; Zhulina, E. B. *Polymer* **1984**, *25*, 1453.
(15) Zhulina, E. B.; Birshtein, T. M. *Polym. Sci. USSR* **1985**, *27*, 570. Birshtein, T. M.; Zhulina, E. B. *Polymer* **1989**, *30*, 170.
(16) Halperin, A. *Macromolecules* **1987**, *20*, 2943.
(17) Zhulina, E. B.; Birshtein, T. M.; Priamitsyn, V. A.; Klushin, L. I. *Macromolecules* **1995**, *28*, 8612.
(18) Fleer, G. J.; Cohen Stuart, M. A.; Scheutjens, J. M. H. M.; Cosgrove, T.; Vincent, B. *Polymers at Interfaces*; Chapmann and Hall: London, 1993.
(19) We note that the scaling arguments (and diagram) were formulated for structures that display a spherical geometry. On the other hand, the structures that emerge from the 2D SCF have a cylindrical geometry. As a consequence, the onset of pinned micelle formation in the SCF calculations is shifted to higher values of N_B/s. It is for this reason that the SCF calculations reveal a laterally homogeneous layer at $N_B = 20$, $\rho = 0.025$, and small values of N_A, while the scaling diagram predicts the formation of pinned micelles.
(20) Li, W.; Balazs, A. C. *Mol. Simul.* **1994**, *13*, 257.
(21) Gersappe, D.; Fasolka, F.; Jacobson, S.; Balazs, A. C. *J. Chem. Phys.* **1994**, *100*, 9170.
(22) Zhulina, E. B.; Vilgis, T. M. *Macromolecules* **1995**, *28*, 1008.

MA9606420